EPJ Web of Conferences **270**, 00024 (2022) https://doi.org/10.1051/epjconf/202227000024
QCD@Work 2022

The axion potential in quark matter

M. Ruggieri[1], *D.E.A.* Castillo[2], *A.G.* Grunfeld[3], and *Bonan* Zhang[1]

[1]School of Nuclear Science and Technology, Lanzhou University, 222 South Tianshui Road, Lanzhou 730000, China
[2]Institute of Nuclear Physics, Polish Academy of Sciences, Radzikowskiego 152, 31-342 Cracow, Poland
[3]CONICET, Godoy Cruz 2290, C1425FQB Ciudad Autónoma de Buenos Aires, Argentina *and* Departamento de Física, Comisión Nacional de Energía Atómica, Av. Libertador 8250, C1429 BNP, Ciudad Autónoma de Buenos Aires, Argentina

Abstract. We study the QCD axion potential in hot and dense quark matter, within an NJL-like model that includes the coupling of the axion to quarks. Firstly we compute the effect of the chiral QCD crossover on the axion mass and self-coupling. Then, we compute the axion potential and study the domain walls. We find that the energy barrier between two adjacent vacuum states decreases in the chirally restored phase: this results in a lower surface tension of the walls. Finally we comment on the possibility of abundant production of walls in hot and dense quark matter.

1 Introduction

Axions are hypothetical particles whose existence was suggested by Peccei and Quinn to solve the strong CP problem [1, 2]. The existence of this particle has not been either proven or disproven, therefore it is still interesting to study them in extreme environments of large density and high temperature matter. This is the purpose of the study presented here. Within an NJL-like model [3–6] we study the coupling of axions to quarks in quark matter, like the one that could be present in the dense interior of compact stars or that produced in the very young universe before the QCD phase transition happened. In particular, we focus on the determination of the axion potential and its response to the QCD phase transition at large density and/or high temperature. Then, we comment on the possibility of production of axion walls in these extreme conditions.

2 The model

We work in the grand canonical ensemble formalism, using T and μ as state variables, where μ denotes the quark number chemical potential. We consider two flavor quark matter with Lagrangian density given by

$$\mathcal{L} = \bar{q}\left(i\partial\!\!\!/ + \hat{\mu}\gamma_0 - m_0\right) q + \bar{e}\left(i\partial\!\!\!/ + \mu_e\gamma_0\right) e + \mathcal{L}_{\rm int}, \tag{1}$$

Here q denotes the quark field carrying Dirac, color and flavor indices,while e is the electron field. m_0 is the current quark mass, that we take to be equal for u and d quarks for simplicity.

The quark chemical potential matrix is diagonal in flavor space, $\hat{\mu} = \mathrm{diag}(\mu_u, \mu_d)$, with

$$\mu_u = \mu - \frac{2}{3}\mu_e, \quad \mu_d = \mu + \frac{1}{3}\mu_e; \tag{2}$$

$\mu_d = \mu_u + \mu_e$ in agreement with the requirement of $\beta-$equilibrium. The interaction term is

$$\mathcal{L}_{\rm int} = G_1 \left[(\bar{q}\tau_a q)(\bar{q}\tau_a q) + (\bar{q}\tau_a i\gamma_5 q)(\bar{q}\tau_a i\gamma_5 q)\right] + 8G_2 \left[e^{i\frac{a}{f_a}} \det(\bar{q}_R q_L) + e^{-i\frac{a}{f_a}} \det(\bar{q}_L q_R)\right]. \tag{3}$$

In the above equation τ_a are matrices in the flavor space with $a = 0, \ldots, 3$; τ_0 is the identity and τ_i with $i = 1, 2, 3$ are the Pauli matrices, normalized as $\mathrm{tr}(\tau_i \tau_i) = \delta_{ij}/2$. The coupling constant G_1 governs the $U(1)_A-$invariant interaction. Similarly, G_2 regulates the strength of the $U(1)_A-$breaking term; the determinant in the latter is understood in the flavor space.

The thermodynamic potential at one loop has been discussed in the literature, see [3] and references therein; it reads

$$\Omega = \Omega_{\rm mf} + \Omega_{1-\rm loop} + \Omega_e. \tag{4}$$

Here we have put

$$\Omega_{\rm mf} = -G_2(\eta^2 - \sigma^2)\cos(a/f_a) + G_1(\eta^2 + \sigma^2) - 2G_2\sigma\eta\sin(a/f_a), \tag{5}$$

that represents the mean field contribution to Ω, with $\sigma = \langle \bar{q}q \rangle$, $\eta = \langle \bar{\eta} i\gamma_5 \eta \rangle$. Moreover,

$$\Omega_e = -2T\frac{4\pi}{8\pi^3}\left(\frac{7\pi^4}{180}T^3 + \frac{\pi^2\mu_e^2 T}{6} + \frac{\mu_e^4}{12T}\right) \tag{6}$$

is the contribution of the free, massless electrons. Finally, $\Omega_{1-\rm loop}$ corresponds to the quark loop contribution, given by

$$\Omega_q = -4N_c \sum_{f=u,d} \int \frac{d^3p}{(2\pi)^3}\left[\frac{E_p}{2} + \frac{1}{2\beta}\log(1 + e^{-\beta(E_p - \mu_f)})(1 + e^{-\beta(E_p + \mu_f)})\right], \tag{7}$$

with $\beta = 1/T$. The dispersion laws of quarks are given by

$$E_p = \sqrt{p^2 + \Delta^2}, \quad \Delta^2 = (m_0 + \alpha_0)^2 + \beta_0^2, \tag{8}$$

with

$$\alpha_0 = -2\left[G_1 + G_2\cos(a/f_a)\right]\sigma + 2G_2\eta\sin(a/f_a), \tag{9}$$

$$\beta_0 = -2\left[G_1 - G_2\sin(a/f_a)\right]\eta + 2G_2\sigma\sin(a/f_a). \tag{10}$$

The electron chemical potential is fixed for each value of the pair (μ, T) by imposing the electrical neutrality condition

$$\frac{\partial\Omega}{\partial\mu_e} = 0. \tag{11}$$

Moreover, the condensates are computed self-consistently by solving the gap equations

$$\frac{\partial\Omega}{\partial\sigma} = 0, \quad \frac{\partial\Omega}{\partial\eta} = 0, \tag{12}$$

being sure that the solution $\sigma = \bar{\sigma}$, $\eta = \bar{\eta}$ corresponds to the global minimum of Ω. We notice that the first integral in the right hand side of Eq. (7) is ultraviolet divergent: we regulate this divergence by cutting the integration at $p = \Lambda$ and treat Λ as a parameter that we fix by the value of the chiral condensate in the vacuum. The set of parameters we use is $\Lambda = 590$ MeV, $G_0\Lambda^2 = 2.435$, $G_1 = (1 - c)G_0$, $G_2 = cG_0$ with $c = 0.2$, $m_0 = 6$ MeV [3].

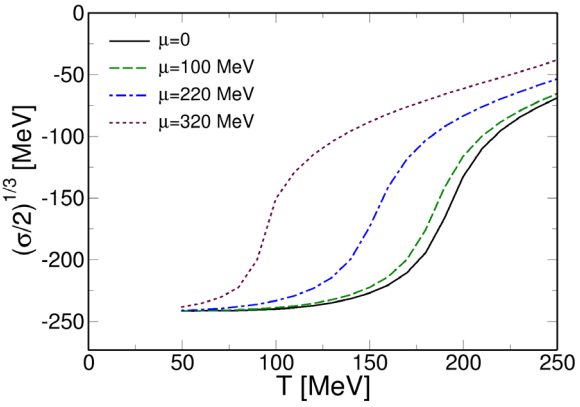

Figure 1. $(\sigma/2)^{1/3}$ versus T for several values of μ in the neutral ground state.

3 Results

In Fig. 1 we plot $(\sigma/2)^{1/3} = (\langle\bar{u}u + \bar{d}d\rangle/2)^{1/3}$ versus T for several values of μ. The chiral condensate drops down in a narrow range of temperature, signaling the approximate restoration of chiral symmetry. This allows us to define a pseudo-critical temperature, T_c, as the temperature where σ has its largest variation. T_c drops as the chemical potential increases. In addition to this, we notice that the variation of σ becomes sharper with μ: the smooth crossover at $\mu = 0$ becomes a sharp transition at at large μ.

The axion potential near the origin is characterized by the mass and the self-coupling,

$$m_a^2 = \left.\frac{d^2\Omega}{da^2}\right|_{a=0}, \quad \lambda_a = \left.\frac{d^4\Omega}{da^4}\right|_{a=0}. \tag{13}$$

At $T = \mu = 0$ we find

$$m_a f_a = 6.38 \times 10^3 \text{ MeV}^2, \quad \lambda_a f_a^4 = -(55.63 \text{ MeV})^4, \tag{14}$$

in agreement with previous estimates [3, 7]. In Fig. 2 we plot the axion mass (left panel) and the self-coupling (right panel) versus T for several values of μ. In correspondence of the QCD crossover the axion mass drops significantly. Moreover, increasing μ results in a sharper drop of the axion mass, similarly to what happens to the chiral condensate.

The fact that $\lambda_a < 0$ means that the quartic interaction is attractive. We notice that in correspondence of the chiral crossover, the quartic coupling experiences a kink that becomes more pronounced when the crossover becomes sharper, namely when the critical endpoint is approached. Thus, despite the fact that λ_a tends to become smaller with T, the chiral crossover enhances the axion self-coupling and this enhancement is very pronounced in proximity of the critical endpoint.

Next we turn to the full axion potential (4). In the left panel of Fig. 3 we plot the axion potential versus a/f_a for several values of μ and for $T = 10$ MeV; this has been computed along the neutrality line (11). Increasing μ results in the lowering of the barrier between the two degenerate vacua $a = 0$ and $a/f_a = 2\pi$.

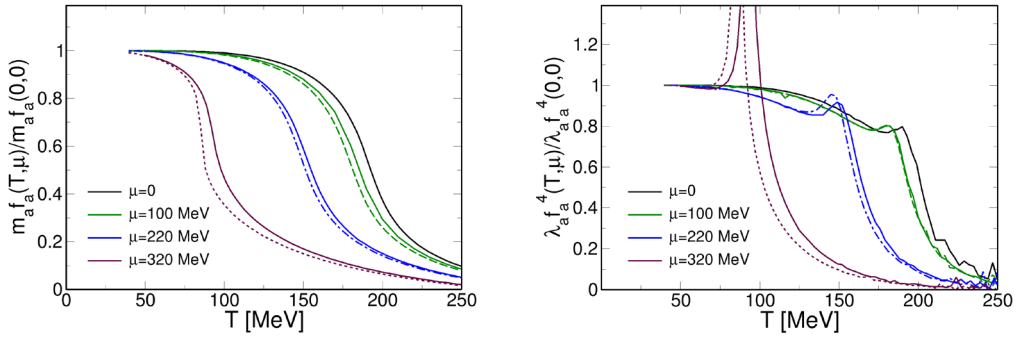

Figure 2. $m_a f_a$ versus T (left panel) and $\lambda_a f_a^4$ (right panel) for several values of μ. Solid lines correspond to the calculations with electrical neutrality while dashed lines denote the results for $\mu_e = 0$.

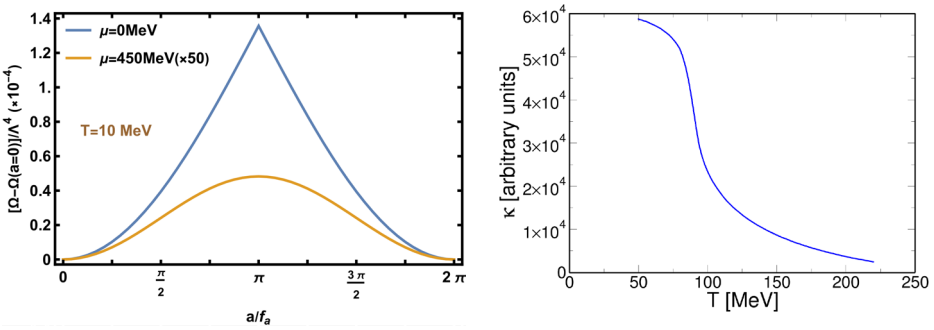

Figure 3. Axion potential $T = 10$ MeV (left panel), and surface tension of the axion walls versus T at $\mu = 320$ MeV (right panel).

The potential shown in Fig. 3 gives rise to domain walls that interpolate between two successive vacua, because the potential is invariant under the discrete symmetry transformation $\theta \to \theta + 2\pi n$ with $\theta \equiv a/f_a$ and $n \in Z$, while this symmetry is broken spontaneously by choosing one value of θ, for example $\theta = 0$. Since the energy barrier between two adjacent vacua decreases in the chirally restored phase, the energy stored in the domain walls also decreases in this phase. The domain wall solution can be built up following well known procedure of classical field theory, starting with the lagrangian density

$$\mathcal{L} = \frac{1}{2}\partial^\mu a \partial_\mu a - V(a/f_a), \quad V(\theta) = \Omega(\theta) - \Omega(0). \tag{15}$$

We checked that in the chirally restored phase a good approximation to the potential is given by

$$V(\theta) = V_0(1 - \cos\theta) = m_a^2 f_a^2 (1 - \cos\theta); \tag{16}$$

for this potential, the solution representing a domain wall at rest is

$$\theta_{\pm}(\xi) = 4 \arctan \exp\left(\pm m_a x\right). \tag{17}$$

m_a corresponds to the in-medium axion mass computed self-consistently within the NJL model. In the chirally broken phase, the potential and the domain wall solutions have to be computed numerically solving the equation of motion arising from the lagrangian density (15). The energy per unit of transverse area of the time-independent domain wall is

$$\kappa \equiv \frac{E}{L^2} = \int_{-\infty}^{+\infty} dx \left[\frac{1}{2}\left(\frac{da}{dx}\right)^2 + V(a/f_a)\right]. \tag{18}$$

The surface tension versus temperature is shown for $\mu = 320$ MeV in the right panel of Fig 3. Around the phase transition, κ decreases as anticipated. It is useful to notice that the energy cost of adding one axion wall to bulk quark matter is κL^2. This has to be compared with the free energy of the bulk quark matter. In the thermodynamic limit, $L \to \infty$, the energy of the background of quark matter is $\propto L^3$. Accordingly, the free energy cost of adding one of these solitons to the bulk of quark matter is zero in this limit. Consequently, we expect an abundant production of axion walls in dense/hot quark matter. The study of the properties of these walls, as well as of their potential observable effects, will be the subject of future studies.

4 Conclusions

We studied the potential of axions on hot and/or dense quark matter, within an NJL-like model; this model has a phase transition to a chirally restored phase at high temperature and/or large density, hence it allows us to study the coupling of axions to quarks both in the confinement and in the deconfinement phases, and the feedback of the QCD crossover on the axion potential. We found that the potential is very sensitive to the crossover, in particular for large values of μ where the crossover is sharp and eventually becomes a real second order phase transition at the critical endpoint. We also analyzed the surface tension, κ, of the axion walls in the hot/dense quark matter. We found that κ decreases in the chirally restored phase. Moreover, we noticed that in the thermodynamic limit, adding a wall to the bulk of quark matter has a zero energy cost, therefore we expect abundant walls production in this environment.

M. R. acknowledges the organizers of QCD@Work for their kind hospitality; moreover, he acknowledges discussions with Mark Alford, Efrain Ferrer and Vivian Incera during the conference, John Petrucci for inspiration, Z. Y. Lu for numerous discussions and S. S. Wan for his support on the initial part of this project. M. R. is supported by the National Science Foundation of China (Grants No.11805087 and No. 11875153). A. G. Grunfeld would like to acknowledge CONICET for financial support under Grant No.PIP17-700.

References

[1] R. D. Peccei and H. R. Quinn, Phys. Rev. Lett. **38**, 1440-1443 (1977) doi:10.1103/PhysRevLett.38.1440

[2] R. D. Peccei and H. R. Quinn, Phys. Rev. D **16**, 1791-1797 (1977) doi:10.1103/PhysRevD.16.1791

[3] Z. Y. Lu and M. Ruggieri, Phys. Rev. D **100**, no.1, 014013 (2019) doi:10.1103/PhysRevD.100.014013 [arXiv:1811.05102 [hep-ph]]

[4] S. B. Ruester, V. Werth, M. Buballa, I. A. Shovkovy and D. H. Rischke, Phys. Rev. D **72**, 034004 (2005) doi:10.1103/PhysRevD.72.034004 [arXiv:hep-ph/0503184 [hep-ph]]
[5] D. Blaschke, S. Fredriksson, H. Grigorian, A. M. Oztas and F. Sandin, Phys. Rev. D **72**, 065020 (2005) doi:10.1103/PhysRevD.72.065020 [arXiv:hep-ph/0503194 [hep-ph]]
[6] D. N. Aguilera, D. Blaschke, M. Buballa and V. L. Yudichev, Phys. Rev. D **72**, 034008 (2005) doi:10.1103/PhysRevD.72.034008 [arXiv:hep-ph/0503288 [hep-ph]]
[7] G. Grilli di Cortona, E. Hardy, J. Pardo Vega and G. Villadoro, JHEP **01**, 034 (2016) doi:10.1007/JHEP01(2016)034 [arXiv:1511.02867 [hep-ph]]